Barrierless Hyper-fast Molecular Rotors in the Gigahertz Regime at 2K Engineered in Metal Organic Frameworks

Jacopo Perego, Silvia Bracco, Mattia Negroni, Charl Bezuidenhout, Giacomo Prando, Pietro Carretta, Angiolina Comotti,* Piero Sozzani*

Department of Materials Science, University of Milano Bicocca, Via R. Cozzi 55, 20125 Milan, Italy

and

Department of Physics, University of Pavia, Via A. Bassi 6, 27100 Pavia, Pavia, Italy

Email: piero.sozzani@unimib.it

Email: angiolina.comotti@unimib.it

ABSTRACT

In the organic matter dynamic and fluid phases cannot survive down to temperatures of a few kelvins, temperature at which only low-inertial-mass groups, such as methyls, may exhibit fast rotation. Here we fabricate 3D-architectures of spontaneous molecular rotors by engineering in metal organic frameworks full-fledged barrierless rotors with exceptionally-low activation energy of 6.2 small cal mol^{-1}. The trigonal bipyramidal symmetry of the rotator in the struts was frustrated by its arrangement in the cubic crystal cell, generating high multiplicity of 12 shallow minima per turn, with a benchmark 10^{10} Hertz frequency persistent even below 2K. The nearly degenerated energy landscape allows for continuous unidirectional hyper-fast rotation, which lasts for hundreds of turns, by 'overflying' several minima. Such an impressive dynamic performance in solid organic matter is only comparable to that of methyl rotation, opening new fields of application whenever hyper-fast dynamics at extremely-low temperatures and minimization of thermal-noise are needed.

INTRODUCTION

Molecular-dynamics phenomena are ubiquitous in nature, and often participate in the fundamental mechanisms of living systems.[1-5] Generally, fluid phases support such phenomena while solid phases are universally considered to be the least suitable to sustain fast molecular motion. However, in solids, molecular moieties can be permanently set apart, one from the other, preventing mutual interactions and promoting unusual internal dynamics. This behavior takes place in low-density solids where non-interacting moving elements can be engineered.[6-13] In reality, dynamics in solid phases can cross the realm of liquid and gaseous phases, leading to unusual phenomena such as high thermal capacity, low surface friction and unexpected physical and chemical properties.[14,15] In recent years molecular rotors, motors and switches in the solid state have been recognized as posing a major challenge, although for an effective translation of molecular dynamics into useful properties, the organization of rotating elements in the solid state or on surfaces appears the winning strategy.[16-21]

The application of porous materials in this field of rotary motion can be regarded as a step forward in the endeavour to gain complete control over motional properties: indeed, porous materials combine a large free-volume that promotes disentangled rotator revolution, allowing pore accessibility to chemical species that intervene in rotary mechanics.[22-28] Thus, rotor-containing porous materials provide a platform for the construction of ultra-fast reorienting elements in a robust framework: an effective strategy for engineering dynamically responsive materials.

Here we pursue these goals by fabricating two new metal organic frameworks (MOFs) with benchmark mobility, containing a bicycle-di-carboxylate linker. Indeed, the construction of supramolecular architectures by simple struts containing rotary masses with the lowest molecular-mass limit produces molecular rotors as fast as $8*10^9$ Hz at 2 K, a rotatory speed at 2 K never before described for any organic moiety in the solid state. Hyperfast molecular rotor dynamics were provided by the extraordinary torsional flexibility of pivotal bonds and the mismatch of the rotator trigonal symmetry with a crystal arrangement, modulated by the metal-nodes, resulting in the frustration of energy minima during the rotational trajectory (Frustrated Trigonal-symmetry Rotator: FTR). The 3D arrays of rotors were realized by the spontaneous self-organization of an aliphatic yet rigid building block (bicycle-di-caboxylic acid) and Zn or Zr clusters, forming Zn-FTR and Zr-FTR compounds, respectively. The absence of either contact or long-range interactions among rotors in Zn-FTR flattens carbon-carbon torsional energy barriers to a limit of less than 6.2 small calories per mole, lower than thermal energy even at liquid-He temperature. The 3-fold symmetry axis of the rotator, conflicting with the 4-fold symmetry axis of the pivotal carboxylates anchored to the metal cluster, frustrates the formation of stable conformations and originates 12 torsional energy minima per turn, with a small displacement of only 15° between a minimum and the next maximum. This striking discovery was

made possible by ^{1}H NMR spin lattice relaxation T_1 times recorded down to very low temperatures such as 1.5 K. Measurements of the spin-lattice relaxation times at distinct magnetic fields (from 0.66 to 7 Tesla) show the characteristic field independent behaviour expected in the fast motional regime, where the dynamics are much faster than the nuclear Larmor frequency (0.3 GHz at 7 Tesla). Molecular dynamics simulations gave an insight into the rotary mechanism and recognized durable runs of hyperfast unidirectional continuous rotation, rarely stopping in a single energy well.

RESULTS AND DISCUSSION

Structure and porosity of the MOF crystals. Zn-MOF was obtained by self-assembly at room temperature of the bicyclo [1.1.1] pentane-1,3-dicarboxylic acid ligand with Zn ions in DMF while Zr-MOF was obtained by a solvothermal synthesis modulated by formic acid to control the crystallization process. Porous crystalline architectures were obtained after gradual solvent exchange and activation under vacuum at 130° and 140 °C, respectively. Nanosize crystals of cubic and octahedral morphology were observed for Zn-FTR and Zr-FTR, respectively, as shown in SEM micrographs (Supplementary Figures 4 and 5). The powder XRD patterns were consistent with highly ordered crystalline porous materials, and the crystal structures were refined by the Rietveld method combined with molecular mechanics and plane-wave DFT calculations (Supplementary Figures 6 and 7). Cubic crystal structures for Zn-FTR and Zr-FTR with space groups of *F*-43*c* and *F*32, respectively, were obtained (Figure 1). The metal node in compound Zn-FTR comprises 4 zinc ions organized in tetrahedral clusters, coordinating 6 carboxylates bridging zinc pairs.[29] Comparatively, the use of Zr dramatically changes the coordinative arrangement: 12-coordinated ligands spring from the nodes, forming a crowded arrangement.[30,31] The IR spectra indicate that after coordination with Zn and Zr ions, C=O stretching bands of the carboxylate shift from 1684 cm^{-1} in the free ligand to 1609 and 1580 cm^{-1}, respectively (Supplementary Figure 8). The number of three signals in ^{13}C MAS NMR spectra is consistent with the high symmetry of the unit cells (Supplementary Figure 9s).

Zn-FTR contain pores that can host spheres of 10.6 Å diameter, whilst Zr-FTR exhibits two smaller tetrahedral and octahedral cavities of 4.0 and 8.6 Å (Figure 1B,E). The porosity of two MOFs was demonstrated by N_2 isotherms, displaying Langmuir type I profiles, at 77 K (Supplementary 11 and 12). The high surface area of 2700 m^2/g and a pore volume of 1.17 cm^3/g demonstrated the remarkable porosity of Zn-FTR: the pore size distribution is centred at 11.8 Å, in agreement with the pore sizes from the crystal structures.

In the crystal structure the three methylenes of the bi-cyclopentane rotator lie on a common plane arranged as a wheel mounted on the main molecular axis of the ligand (Figure 1C): any wheels in Zn-FTR set their hydrogen atoms at distances of 7.9 Å and 5.4 Å from the next neighbouring rotor

hydrogens. Consequently, they do not interfere with each other or with any other moiety in the rotary dynamics. The distances are shorter among the rotors in Zr-FTR (3.3 Å), but are still longer than the van der Waals contacts.

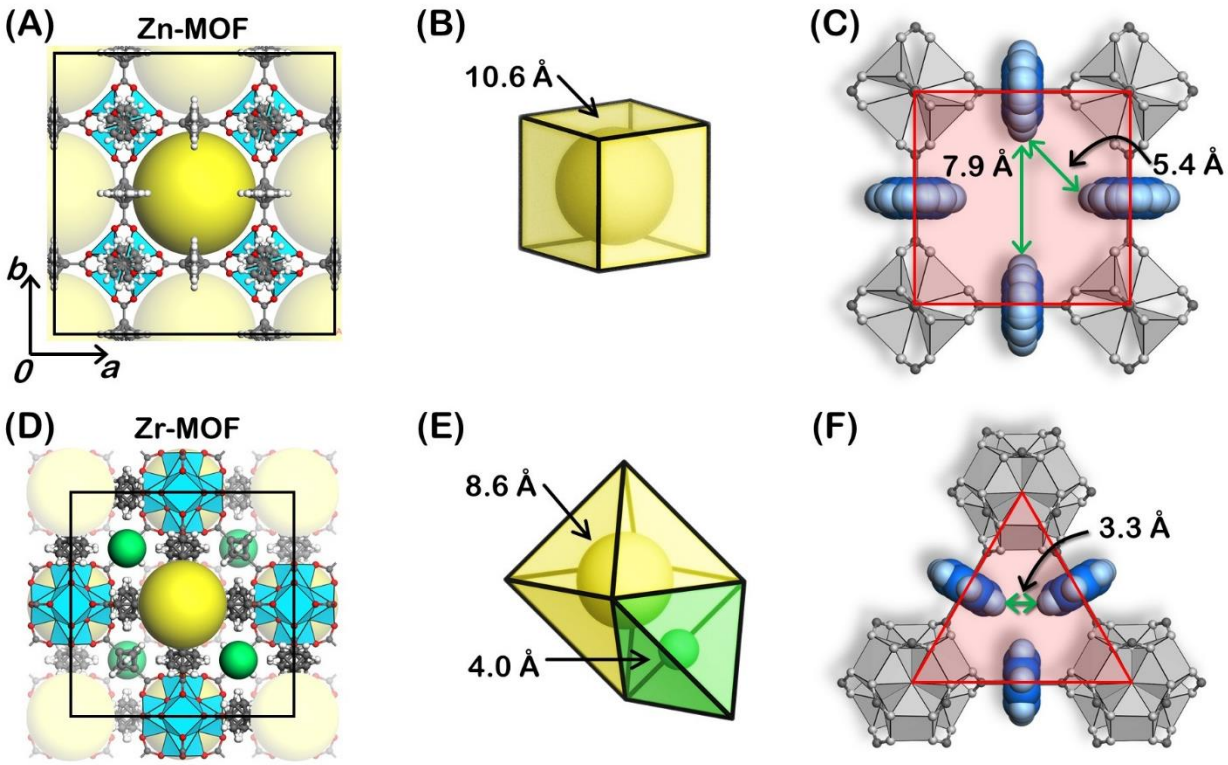

Figure 1. (A, D) The crystal structures of Zn-MOF and Zr-MOF viewed along the *c*-axis. The metal-oxide nodes are shown in the polyhedron representation. (B, E) The schematic geometries of the pores for both MOFs as well as the largest spheres that can be accommodated within the pores. The diameters of the spheres are indicated on the figure. Shortest distances between the rotor hydrogen atoms, as calculated from the center of the nuclei for Zn-FTR (C) and Zr-FTR (F).

Rotor Conformations and energy landscape. A key point of the MOF crystal structure is that the carboxylate planes in Zn-FTR are set perpendicular to one another (crossed arrangement) while in Zr-FTR the carboxylate groups lie on a common plane (in-plane arrangement) (Figure 2A,B). *Ab initio* conformational analysis of the dicarboxylate-bicyclopentane showed the crossed arrangement as more stable by 0.39 kcal/mol than the in-plane arrangement (Supplementary Figure 13): however, the anchorage of the ligands to the metal nodes prevents conversion between arrangements in the structures. These arrangements have dramatic consequences on the energetics of the central rotator. The torsional conformations were investigated by MP2 potential energy scans, displaying minima every 60° (sixfold rotation axis) for the in-plane arrangement, while the energy minima occurred with a period of 30° (twelvefold rotation axis) for the crossed arrangement (Figure 2C,D and

Supplementary Figure 14). In both cases the energy barriers, as calculated by MP2/6-311++G(d), are of a few small calories per mole. The energy barrier of in-plane conformation is accounted for 50 cal mol^{-1}, while in crossed arrangement it was found to be lower than a few calories per mole and comparable to the thermal agitation at 0.5 K (Figure 2E), showing the extremely-high torsional flexibility of the rotator, comparable to methyl rotation flexibility.[32-35] The in-plane and crossed arrangements of the two carboxylate groups in the ligand are characteristic of the crystal structures with Zr and Zn metal nodes, respectively, thus, it is expected that the molecular wheels in Zn-FTR will exhibit extremely high mobility.

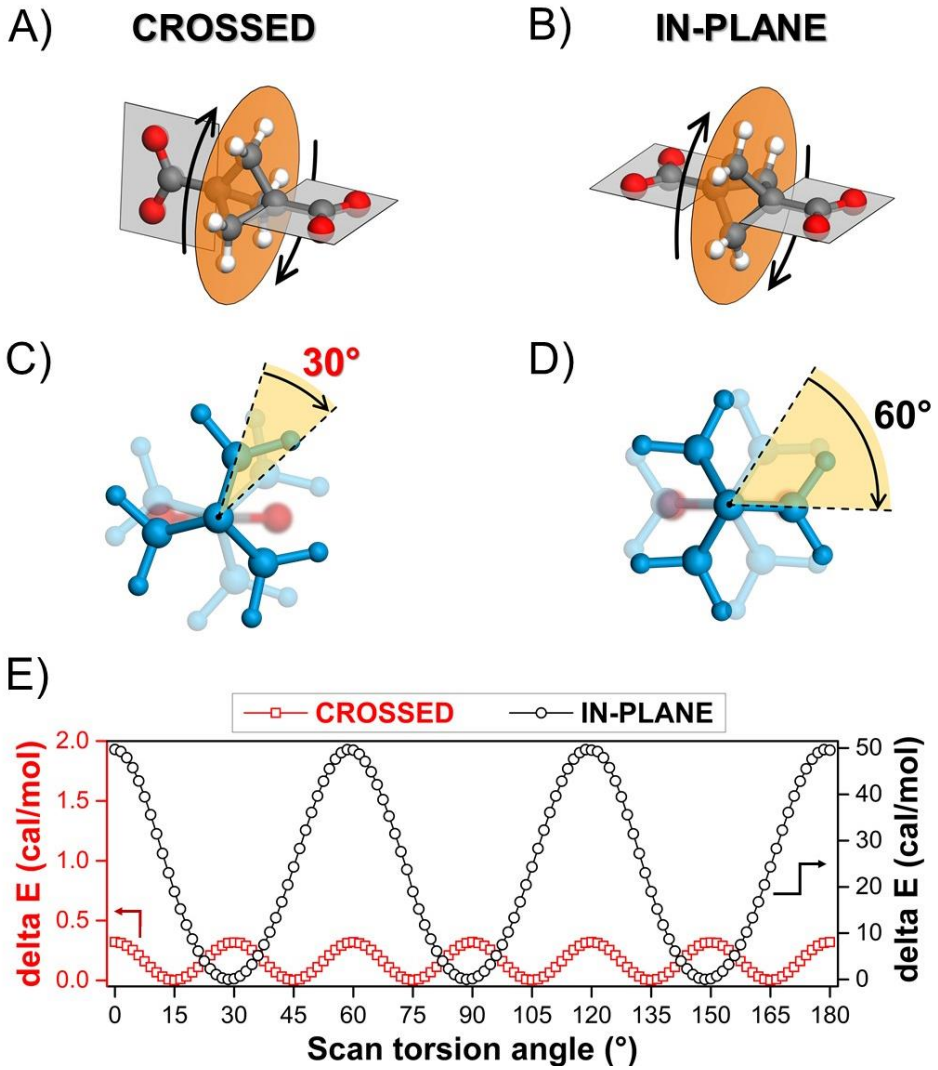

Figure 2. Rotor minimum conformations for A) crossed and B) in-plane arrangements as in Zn-FTR and Zr-FTR, respectively. C) and D) Conformational minima for the crossed and in-plane arrangements occurring by rotations of 30° and 60°, respectively. E) An overlay of the crossed (red squares) and in-plane (black circles) potential energy scans (PES) plotted from 0 to 180° with separate y-axes scales (crossed on the left in red and in-plane on the right in black).

Hyperfast rotor dynamics by NMR at 2K-298K and 0.6T-7T magnetic fields. A unique tool to provide the evidence of dynamics in crystalline matter is variable-temperature solid-state NMR

spectroscopy. ^{13}C NMR spectra of Zn-FTR, recorded without spinning, exhibited pseudo-isotropic signals for methylenes, both at room temperature and down to 163 K, showing narrow lines of 1.4 and 2 ppm, respectively, thus depicting rotary revolution, fast enough to average out chemical-shift-anisotropy (CSA) (Figure 3A).[36] For comparison, Figure 3A (black line) shows the full CSA profile determined by *ab initio* GIAO calculations, consistent with the reference bicyclopentane hydrocarbon CSA. The mixing of the principal tensor-components in the x-y plane orthogonal to the rotor axis (σ_{xx} = 44 ppm and σ_{yy} = 60 ppm, Figure 3B) produces an averaged value of 52 ppm, equal to the σ_{zz} component, which is unaffected by rotator reorientation, being parallel to the rotation axis. Such an extreme restriction of CSA to isotropic lines in the solid-state occurs only in globular molecules, such as adamantane and fullerene, that display linewidths of 5 ppm at 298 K and of 2.4 ppm at 190 K, respectively, although in these cases phase transitions prevent fast dynamics at lower temperature.[37,38] For comparison, at 163 K the crowded Zr-MOF showed a residual CSA profile and a 4.4 ppm linewidth, with a prominent peak corresponding to the mixing of σ_{xx} and σ_{yy}, and a lateral signal for the σ_{zz} component (Figure 3C). The identification of an σ_{zz} separate component, not mixed with the remaining tensors, clearly highlights the axial symmetry of the rotary trajectories.

From the hydrogen nucleus viewpoint, solid-state NMR spectra of Zn-FTR displayed 16 kHz-wide methylene signals (Figure 3D), which appear markedly modulated by through-space homonuclear dipolar couplings even at 2 K. The unusual ^{1}H NMR spectrum patterning was successfully simulated by considering the orientation and distance dependence of the dipole-dipole interactions in the 6-spin cluster of an individual rotor under magnetic and molecular isolation. The spectra are substantially a combination of Pake spectra containing the anisotropic information and dynamical averaging among hydrogens in the rotator plane (Supplementary Figure 16). A similar 6-nuclei modulated spectrum has only been investigated in fast-spinning benzene within a graphite layer.[39] An orbital trajectory of hydrogen nuclei, perpendicular to the rotor main axis in the fast motion limit ($>10^8$ Hz), was demonstrated by the overall line-shape restriction of the full 'static' powder pattern to be half of its width. Furthermore, taking into account hydrogen-hydrogen dipolar interactions in the crystal cell, we evaluated the second moment and demonstrated that 98% of the effective interactions occur within the six methylene hydrogens of each rotator (Figure 3D and Supplementary Figure 17).[40] Importantly, from this evaluation it was possible to calculate the relaxation constant C of $5.8*10^9$ s^{-2} (proportional to the mean square amplitude of the fluctuating field at the nuclei), which is used below to establish the correlation times from NMR spin-lattice relaxation times.

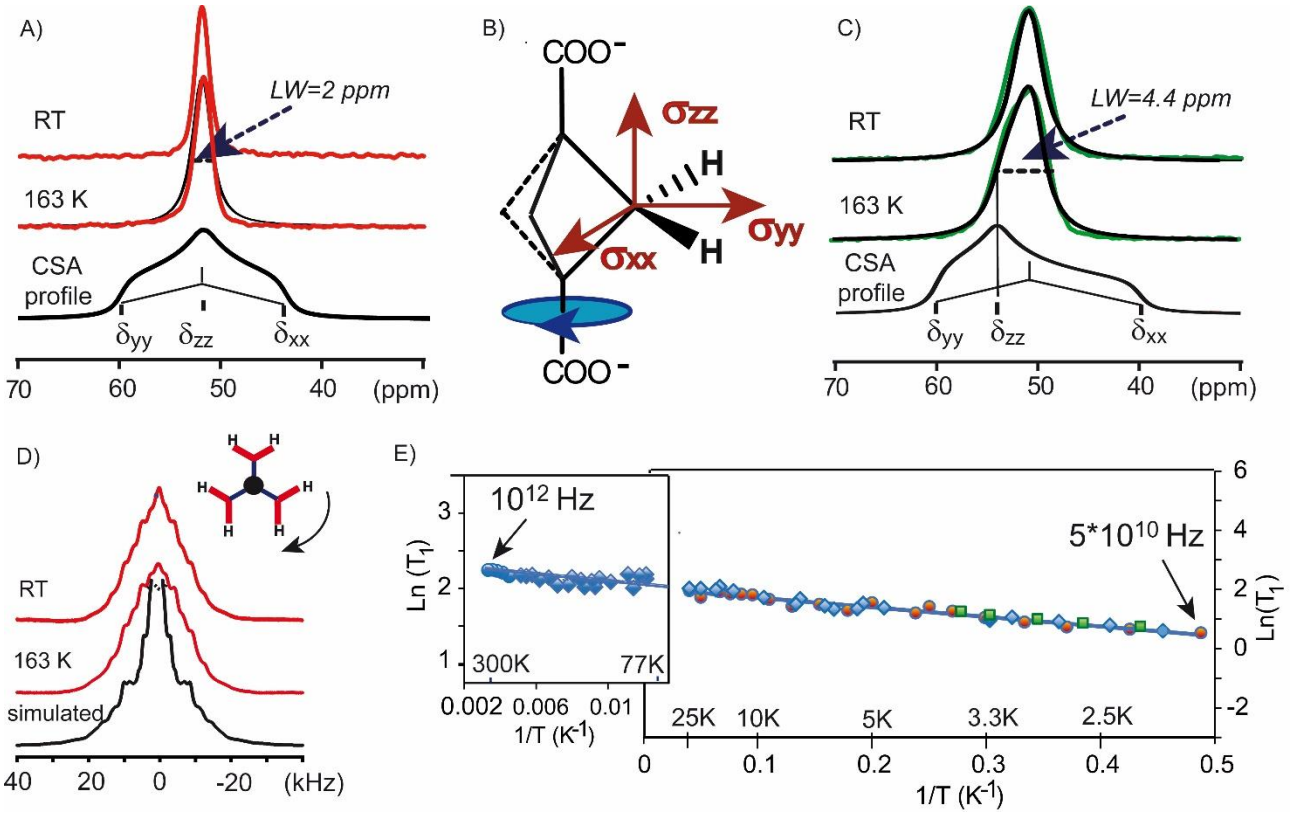

Figure 3. ^{13}C CP NMR spectra of Zn-FTR (A) and Zr-FTR (B) at room temperature, at 163 K and CSA profiles as calculated by considering fast rotation of CH_2 about their main axis. B) Chemical structure of dicarboxylate-bicyclopentane and the main components of the ^{13}C CSA tensor. D) ^{1}H NMR spectrum of Zn-FTR at room temperature, at 163 K and the simulated pattern considering the dipolar couplings among a cluster of six hydrogens, as in an isolated bicyclo-based molecule. E) ^{1}H T_1 relaxation times versus the reciprocal of temperature in the temperature range from 1.5 to 300 K. The T_1 relaxation times were measured at 7.04 (blue circle), 1.66 (green square), 1.0 (blue diamond) and 0.66 T (orange circle).

Solid-state NMR relaxation times are invaluable parameters to explore material dynamics and, collected at various resonance frequencies, encompass reorientation rates of several orders of magnitude. ^{1}H T_1 relaxation times of the bicyclopentane methylenes in Zn-FTR were measured from 298 K down to 1.5 K at a few distinct main magnetic fields B_0 equal to 7.04, 1.66, 1.00 and 0.66 T (Figure 3E: 70 points were collected). The relaxation times were plotted as $\ln T_1$ *vs* 1/T and fitted by the universal master-curve, according to the Kubo-Tomita theory (K-T).[41] Remarkably, such a plot exhibited a field-independent linear decrease with inverse temperature and a constant slope over the entire range (Figure 3E; the 77-298 K range is expanded for clarity). This indicates that the relaxation times are determined by dynamics much faster than the nuclear Larmor frequency, even at extremely low temperature. The barrier for rotation resulted in a value as low as 6.2 cal mol^{-1} (26 J mol^{-1}) for Zn-FTR. The extraordinarily low activation-energy value supports the discovery of an unprecedented molecular rotor with almost negligible energy barriers for rotation. By taking into account the previously determined relaxation constant C, the correlation times can be established for each

temperature. Importantly, the correlation time at infinite temperature τ_0 of $4*10^{-12}$ s^{-1}, is fully consistent with the inertial mass of the rotator (42 mass-units)[42]: further proof that the 'molecular wheels' are operating as individual and independent rotating entities.

Hyper-fast rotary motion of k=37 GHz ($1/\tau_c=2.3*10^{11}$ s^{-1}) at room temperature, and still in the GigaHertz regime ($k=7.9*10^9$ Hz and $1/\tau_c=5.0*10^{10}$ s^{-1}) at temperatures as low as 2 K was established. Such a benchmark energy-barrier of rotary dynamics allows $k=7.3*10^7$ Hz ($1/\tau_c=4.5*10^8$ s^{-1}) rotation to occur at a temperature as low as 0.5 K. To the best of our knowledge, fast molecular rotors in organic matter have not been observed at the liquid helium temperature and below, because the energy barrier is prohibitively high for thermal energy to compete and quenches the rotation (less than 1 Hertz).[13,24] The impressive dynamics here shown is comparable to the fastest conceivable rotation speed among organic moieties at low temperature, such as methyl groups, in the solid and even in the gas phase.[31-35] The strikingly low barrier suggests that not only does the rotor symmetry frustration ensure full-fledged barrierless 'mechanical' flexibility, but also that the framework was engineered as light, yet robust, to support rotors that behave as isolated entities.

Modulation of rotor-speed by crystal-structure and gas-phase action. The observation of the same bicyclopentane rotor in the crowded Zr-FTR structure, which imposes a diverse symmetry and density, could probe the effect of the crystal environment on the rotor freedom, yielding a higher energy barrier of 400 cal mol^{-1} for rotation (Supplementary Figure 25). A modulation effect was also produced by the influence of a gaseous species, which interacts with the rotors accessible through the open pores, rendering feasible an active intervention of the gas phase to tune the hyper-dynamic rotors in the porous Zn-FTR. Indeed, the rotors were regulated by I_2 molecules diffusing spontaneously into the porous crystals at 27 mbar vapour pressure, at 293 K. The rotary speed was drastically reduced, but was still within the *extreme narrowing* motional regime: the activation energy increased to 1000 cal mol^{-1} i.e. three orders of magnitude larger than the empty matrix (Supplementary Figure 25). This increased activation energy from a negligible value was ascribed to a 'weak' favourable interaction of the C-H peripheral methylenes of the rotor-wheel, exposed to the empty volume with iodine molecules, thus probing the sensitivity of the material for any minimal perturbation, useful as a prompt and reversible detector.

Molecular dynamics simulations of unrestricted rotary motion in the crystals. Molecular dynamics simulations constituted a winning strategy, providing a deeper insight into the statistics of the functioning of molecular wheels (Figure 4). The rotation of the rotors was determined by analysing the evolution of their rotatory torsion angles with respect to time. In both compounds the rotor axis oscillations (nutation) are not larger than 3° at any temperature (Supplementary Figure 26).

The robustness of the double anchorage firmly supports the axel to the framework, unlike a methyl rotor, which is mono-dentate and is thus pivoted only on one side.[34,43] The cumulative angular displacement of the rotors at room temperature, shown in number of turns, is depicted in Figure 4B for three selected rotators in Zn-FTR. Clockwise or counter-clockwise rotation can be differentiated by positive or negative angular displacement. A first striking observation was that the rotator neither resides in a single energy minimum, oscillating therein, nor does it move stepwise by jumping from one minimum to the next. Conversely, a multiple-turn displacement, overflying a large number of energy minima (up to 4000 minima, 12 minima are equal to 1 turn) in a single *flight*, was observed. The molecular wheel appears to spin freely and performs a diffusional motion, overriding negligible minima for up to 500 continuous unidirectional revolutions in either clockwise or counter-clockwise directions, depicting a waving behavior as shown in Figure 4B and C. By representing the rotation angles explored by an individual rotator in a 0° - 360° scale against time, the signature of the continuous motion becomes imprinted as parallel noiseless lines (Figure 4D). The rotary speed can be sampled by the average slope (the derivative of the cumulative angle versus time) over several turns in a lasting continuous rotation, and was as fast as 4.5 10^{11} Hz (Figure B and C). This value matches the correlation time τ_0 of $4.3*10^{-12}$ s, measured experimentally by NMR relaxation and Kubo-Tomita analysis.

At low temperature, the rotors possess lower thermal energy and can be trapped occasionally in potential energy wells (Figure 4E). The rapid intermittent stop-and-go behaviour and the persistence at low temperature of hyper-fast rotation manifested in continuous unidirectional motion (Figure 4F and G), suggest that the rotor explores energetic states higher than the tiny energy barrier, even at 2.5 K. The direction can be easily recognized in each free-rotation packet by the positive or negative inclination of the parallel lines. By comparison, Zr-FTR, characterized by a higher barrier, shows frequently-occurring conventional jumps from one energy-well to the next one (Supplementary Figures 33, 34 and 40).

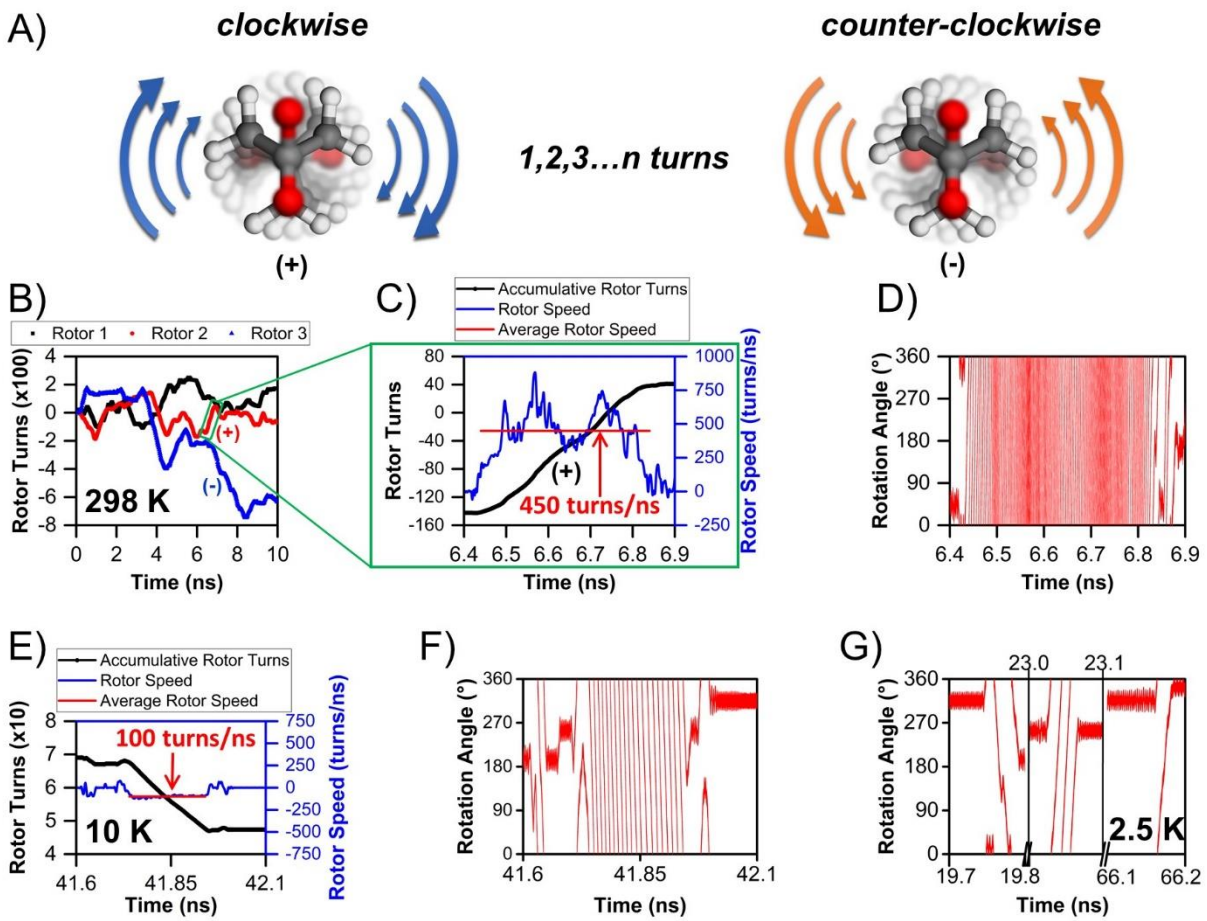

Figure 4. Molecular Dynamics results for Zn-FTR calculated at various temperatures. A) An illustration of clockwise and counter-clockwise rotation of the bicyclo rotating moiety. B) The time evolution of the cumulative torsion angular displacement for the rotors at 298 K. An enlarged section (0.5 ns) of the 298 K dynamics simulation highlighting a continuous movement section (black line), the associated angular speed (blue line) and the average speed (red line). D) The 298 K rotor angular displacement represented in a 0° – 360° scale for the 0.5 ns time window. E) A section of the 10 K dynamics simulation highlighting a continuous movement section (black line), the associated angular speed (blue line) and the average speed (red line) during the 0.5 ns time period. F) The 10 K rotor angular displacement represented in a 0° – 360° scale. G) The 2.5 K rotor angular displacement represented in a 0° – 360° scale showing different time windows of the dynamics simulation.

Conclusion

In conclusion, we realized the fastest low-temperature molecular rotor ever obtained in the solid state. This breakthrough was enabled by the construction of low density architectures of dynamic building blocks, energetically decoupled from their surroundings in crystalline metal organic frameworks. The rotors were isolated one from another in the high-symmetry structure and boasted a negligible torsional barrier to rotation. A key point was the unusual crossed conformation adopted by the carboxylates around the pivotal bond on the rotor axel, generating a 4-fold symmetry that does not match the 3-fold rotation symmetry of the rotator, thus producing geometrical frustration and, for a

full turn, 12 very shallow wells along the circular trajectory. Rotor dynamics have proved faster than simple methyl rotation, which is commonly considered a benchmark for rotor speed, matching the Gigahertz regime at temperatures as cold as 2 K. These noteworthy findings suggest that molecular elements in the solid state, stably connected in a crystalline periodic-order framework, are able to express a hyper-fast rotary motion under very low temperatures because of their engineered 3D arrangement. This remarkable behaviour is the result of the continuous unhindered molecular wheel rotation for several turns, and not the jumping motion usually observed for barrier-restricted rotations. The present discovery demonstrates the existence of dynamic materials under extreme conditions below liquid helium, suggesting future investigations into regular arrays of rotary motors and rotors showing enhanced performance under low thermal perturbation conditions.

Acknowledgements

Financial support from the Italian Ministry of University and Research (MIUR) through the grant "Dipartimenti di Eccellenza-2017 "Materials For Energy" is gratefully acknowledged. This research was funded by the PRIN-2016-NAZ-104 and PRIN-2018 (NEMO) projects.

Author Contributions

A.C., P.S. conceived the study, J.P. designed the materials synthesis and characterization, S.B., G.P., M.N., P. C. carried out NMR measurements and C.B. the theoretical calculations. A.C., P.S. and S.B. co-wrote the manuscript with the suggestions from all the authors. I. Supino is acknowledged for her help during sample preparation.

Competing Interests

The authors declare no competing interests.

Additional information

Supplementary information is available for this paper.

References

1. Saibil, H. Chaperone machines for protein folding, unfolding and disaggregation. *Nat. Rev. Mol. Cell Biol.* **14**, 630-642 (2013).
2. Kinbara, K. & Aida, T. Towards intelligent molecular machines: Directed motions of biological and artificial molecules and assemblies. *Chem. Rev.* **105**, 1377-1400 (2005).

3. Olesen, C. et al. The structural basis of calcium transport by the calcium pump. *Nature* **450**, 1036-1042 (2007).
4. Howard, J., Hudspeth, A. J. & Vale, R.D. Movement of microtubules by single kinesin molecules. *Nature* **342** (1989), 154-158.
5. Preben Morth, J., Pedersen, B. P., Andersen, J. P., Vilsen, B., Palmgren, M. G. & Nissen, P. A structural overview of the plasma membrane Na^+,K^+-ATPase and H^+-ATPase ion pumps. *Nat. Rev. Mol. Cell Biology* **12**, 60–70 (2011).
6. Vogelsberg, C. S. & Garcia-Garibay, M. A. Crystalline molecular machines: function, phase order, dimensionality, and composition. *Chem. Soc. Rev.* **41**, 1892-1910 (2012).
7. Bracco, S., Comotti, A. & Sozzani, P. Molecular rotors built in porous materials. *Acc. Chem. Res.* **49**, 1701-1710 (2016)
8. Danowski, W. et al. Unidirectional rotary motion in a metal-organic framework. *Nat. Nanotech.* **488**, 488-494 (2019).
9. Deng, H., Olson, M. A., Stoddart, J. F. & Yaghi, O. M. Robust dynamics. *Nat. Chem.* **2**, 439-443 (2010).
10. Zhu, K., O'Keefe, C. A., Vukotic, V. N., Schurko, R. W. & Loeb, S. J. A molecular shuttle that operates inside a metal-organic framework. *Nat. Chem.* **7**, 514-519 (2015).
11. Kobr, L. et al. Inclusion Compound Based Approach to Arrays of Artificial Dipolar Molecular Rotors. A Surface Inclusion. *J. Am. Chem. Soc.* **134**, 10122-10131 (2012).
12. Inukai, M., Fukushima, T., Hijikata, Y., Ogiwara, N., Horike, S. & Kitagawa, S. Control of Molecular Rotor Rotational Frequencies in Porous Coordination Polymers Using a Solid-Solution Approach**.** *J. Am. Chem. Soc.* (2015) **137**, 12183-12186.
13. Vogelsberg, C. S. et al. Ultrafast rotation in an amphidynamic crystalline metal organic framework. *Proc. Natl Acad. Sci. USA* **114**, 13613-13618 (2017).
14. Michl, J., Charles, E. & Sykes, H. Molecular Rotors and Motors: Recent Advances and Future Challenges. *ACS Nano* **3**, 1042-1048 (2009).
15. Prokop, A., Vacek, J. & Michl, J. Friction in carborane-based molecular rotors driven by gas flow or electric field: classical molecular dynamics. *ACS Nano* **6**, 1901-1914 (2012).
16. Coskun, A., Banaszak, M., Astumian, R. D., Stoddart, J. F. & Grzybowski, B. A. Great expectations: can artificial molecular machines deliver on their promise? *Chem. Soc. Rev.* **41**, 19-30 (2012).
17. Steuerman, D. W., Tseng, H.-R., Peters, A. J., Flood, A. H., Jeppesen, J. O., Nielsen, K. A., Stoddart, J. F. & Heath, J. R. Molecular-Mechanical Switch-Based Solid-State Electrochromic Devices. *Angew. Chem. Int. Ed.* **43**, 6486-6491 (2004).
18. Collier, C. P., Mattersteig, G., Wong, E. W., Luo, Y., Beverly, K., Sampaio, J., Raymo, F. M., Stoddart, J. F. & Heath, J. R. *Science* **289**, 1172-1175 (2000).
19. Kaleta, J. et al. Surface Inclusion of Unidirectional Molecular Motors in Hexagonal Tris(o-phenylene) cyclotriphosphazene. *J. Am. Chem. Soc.* **139**, 10486-10498 (2017).
20. Jiang, X. et al. Crystal Fluidity Reflected by Fast Rotational Motion at the Core, Branches, and Peripheral Aromatic Groups of a Dendrimeric Molecular Rotor. *J. Am. Chem. Soc.* **138**, 4650-4656 (2016).
21. Comotti, A., Bracco, S., Ben, T., Qiu, S. & Sozzani, P. Molecular Rotors in Porous Organic Frameworks. *Angew. Chem. Int. Ed.* **53**, 1043-1047 (2014).
22. Comotti, A., Bracco, S., Yamamoto, A., Beretta, M., Kirukawa, T. Tohnai, N. Miyata, M. & Sozzani, P. Engineering Switchable Rotors in Molecular Crystals with Open Porosity. *J. Am. Chem. Soc.* **136**, 618-621 (2014)
23. Bracco, S. et al. CO_2 regulates molecular rotor dynamics in porous materials. *Chem. Commun.* **53**, 7776-7779 (2017).
24. Bracco, S. et al. Ultrafast molecular rotors and their CO_2 tuning in MOFs with rod-like ligands. *Chem. Eur. J.* **23**, 11210-11215 (2017).

25. Bracco, S., Beretta, M., Cattaneo, A., Comotti, A., Falqui, A., Zhao, K., Rogers, C. & Sozzani, P. Dipolar Rotors Orderly Aligned in Mesoporous Fluorinated Organosilica Architectures. *Angew. Chem. Int. Ed.* **54**, 4773-4777 (2015).
26. Horike, S., Matsuda, R., Tanaka, D., Matsubara, S., Mizuno, M., Endo, K. & Kitagawa, S. Dynamic Motion of Building Blocks in Porous Coordination Polymers. *Angew. Chem., Int. Ed.* **45**, 7226-7230 (2006).
27. Zhu, K., Vukotic, V. N., Okeefe, C. A., Schurko, R. W. & Loeb, S. J. Metal–organic frameworks with mechanically interlocked pillars: controlling ring dynamics in the solid-state via a reversible phase change. *J. Am. Chem. Soc.* **136**, 7403–7409 (2014).
28. Elsaidi, S.K., Mohamed, M. H., Simon, C. M., Braun, E., Pham, T., Forrest, K. A., Xu, W., Banerjee, D., Space, B., Zaworotko, M. J. & Thallapally, P. K. Effect of ring rotation upon gas adsorption in SIFSIX-3-M (M = Fe, Ni) pillared square grid networks. *Chem. Sci.* **8**, 2373-2380 (2017).
29. Li, H., Eddaoudi, M., O'Keeffe, M. & Yaghi, O. M. Design and synthesis of an exceptionally stable and highly porous metal-organic framework. *Nature* **402**, 276-279 (1999).
30. Cavka, J. H., Jakobsen, S., Olsbye, U., Guillou, N., Lamberti, C., Bordiga, S. & Lillerud, K. P. A New Zirconium Inorganic Building Brick Forming Metal Organic Frameworks with Exceptional Stability. *J. Am. Chem. Soc.* **130**, 13850–13851 (2008).
31. Yuan, S., Qin, J.-S., Lollar, C. T. & Zhou, H.-C. Stable Metal−Organic Frameworks with Group 4 Metals: Current Status and Trends. *ACS Cent. Sci.* **4**, 440-450 (2018).
32. Owen, N. L. in Internal Rotation in Molecules. Ed. Orville-Thomas, W. J. (Wiley, New York, 1974), p. 157.
33. Nakagawa, J. & Hayashi, M. Microwave spectrum and internal rotation of 2-butyne-1, 1, 1-d_3(dimethylacetylene), $CH_3C{\equiv}CCD_3$. *J. Chem. Phys.* 80, 5922 (1984).
34. Ilyushin, V., Rizzato, R., Evangelisti, L., Feng, G., Maris, A., Melandri, S. & Caminati, W. Almost free methyl top internal rotation: Rotational spectrum of 2-butynoic acid. *J. Mol Spectr.* **267**, 186-190 (2011).
35. Hensel, K. D. & Gerry, M. C. L. *J. Chem. Soc. Farad. Trans.* **90**, 3023 (1994).
36. Facelli, J. C., Orendt, A. M., Beeler, A. J., Solum, M. S., Depke, G., Malsch, K. D., Downing, J. W., Murthy, P. S., Grant, D. M. & Michl, J. Low-temperature carbon-13 magnetic resonance in solids. 5. Chemical shielding anisotropy of the $^{13}CH_2$ group. *J. Am. Chem. Soc.* **107**, 6749, 6754 (1985).
37. Gil, A.M. & Alberti, E. The effect of Magic Angle Spinning on proton spin–lattice relaxation times in some organic solids. *Solid State Nuclear Magnetic Resonance.* **11**, 203-209 (1998).
38. Ticko, R., Dabbagh, G., Fleming, R. M., Haddon, R. C., Makhjia, A. V. & Zahurak, S. M. Molecular dynamics and the phase transition in solid C60. *Phys. Rev. Lett.* **67**, 1886-1889 (1991).
39. Panich, A. M. & Panich, E. A. NMR Lineshape of a Six-Spin System with Dipole-Dipole Interactions. Application to Benzene. *J. Magn. Res. Series A* **116**, 113-116 (1995).
40. Goc, R. Computer calculation of the Van Vleck second moment for materials with internal rotation of spin groups. *Comp. Phys. Comm.* **162**, 102-112 (2004).
41. Kubo, R. & Tomita, K. A General Theory of Magnetic Resonance Adsorption. *J. Phys. Soc. J.* **9**, 888-919 (1954).
42. Noel L. Owen, in Internal Rotation in Molecules, edited by W. J. Orville-Thomas (Wiley, New York, 1974), p. 157.
43. Eibl, K., Kannengießer, R., Stahl, W., Nguyen, H. V. L. & Kleiner, I. Low barrier methyl rotation in 3-pentyn-1-ol as observed by microwave spectroscopy. *Molecular Phys.* **114**, 3483-3489 (2016).